entropy

MDPI

Article

Quadratic Growth of Out-of-Time-Ordered Correlators in Quantum Kicked Rotor Model

Guanling Li and Wenlei Zhao *

School of Science, Jiangxi University of Science and Technology, Ganzhou 341000, China; l_guanling@163.com
* Correspondence: wlzhao@jxust.edu.cn

Abstract: We investigate both theoretically and numerically the dynamics of out-of-time-ordered correlators (OTOCs) in quantum resonance conditions for a kicked rotor model. We employ various operators to construct OTOCs in order to thoroughly quantify their commutation relation at different times, therefore unveiling the process of quantum scrambling. With the help of quantum resonance condition, we have deduced the exact expressions of quantum states during both forward evolution and time reversal, which enables us to establish the laws governing OTOCs' time dependence. We find interestingly that the OTOCs of different types increase in a quadratic function of time, breaking the freezing of quantum scrambling induced by the dynamical localization under non-resonance condition. The underlying mechanism is discovered, and the possible applications in quantum entanglement are discussed.

Keywords: quantum scrambling; quantum chaos; kicked rotor

1. Introduction

Quantum scrambling, a fundamental concept elucidating the spread of information across multiple degrees of freedom that is inaccessible via local measurements, has garnered extensive attention in quantum information [1–4], quantum chaos [5–9], and condensed matter physics [10–13]. It is well known that the out-of-time ordered correlators (OTOCs) can quantify the process of information scrambling with relevance to the operator growth [14,15]. The exponential growth of OTOCs, facilitated by exponential instability of chaos, produces the boundary of the light cone of information scrambling in many-body systems [16,17], for which the butterfly velocity of scrambling is closely related to the quantum Lyapunov exponent [18–20]. The relaxation of OTOCs can detect the character of both the quantum thermalization and quantum entanglement in many-body systems [21,22], providing insights into the underlying connection between quantum chaos and information scrambling [23–25]. The dynamics of OTOCs can be used as an order parameter to diagnose phase transitions in both Hermitian [26] and non-Hermitian chaotic systems [27]. Interestingly, genuine quantum chaos, specifically the superexponential instability induced by delta-kicking modulation in nonlinear interactions, can cause the superexponential growth of OTOCs [28], representing a new phenomenon of information scrambling [29,30].

The variants of the quantum kicked rotor (QKR) model under resonance conditions serve as ideal platforms to explore fascinating physics of quantum coherence [31], which has significant implications for the fundamental aspects of quantum transport [32,33] and topological new phases in Floquet systems [34–37]. The existence of the flat band of quasi-energy spectrum determines the exponential diffusion dynamics in the on-resonance double-kicked rotor model [38]. The resonance condition yields Floquet spectrum [39–41] analogous to Hofstadter's butterfly of an integrable system [42–44] and topological phase transitions reminiscent of the integer quantum Hall effect [45,46]. Moreover, a dynamical analog of the integer quantum Hall effect emerges from an intrinsic chaos in spin-1/2 QKR model, enriching our understanding of the quantum topological phenomena induced by

check for updates

Citation: Li, G.; Zhao, W. Quadratic Growth of Out-of-Time-Ordered Correlators in Quantum Kicked Rotor Model. *Entropy* **2024**, *26*, 229. https://doi.org/10.3390/e26030229

Academic Editor: Stefano Mancini

Received: 17 January 2024
Revised: 24 February 2024
Accepted: 1 March 2024
Published: 3 March 2024

chaos [47,48]. Interestingly, the spinor QKR model with quantum resonance condition provides a versatile playground to realize the quantum walk in momentum space [49,50], proposing a new protocol for the manipulation of the quantum transport with Floquet engineering [51]. The state-of-the-art experiments in atom-optics have indeed realized the QKR model and verified the dynamical phase transition and quantum walk therein by precisely tailoring the resonance condition for the driven period [52]. This paves the way for engineering exotic behavior of quantum information [53] and energy diffusion [54] in various generalization of the QKR model.

In this context, we investigate both analytically and numerically the dynamics of different types of OTOCs under the quantum resonance condition. The first type OTOCs C_p involves two angular momentum operators. Furthermore, the second one C_T is constructed by the combination of the translation operator and angular momentum operator. We have derived the exact expression of the quantum state during both forward evolution and time reversal under quantum resonance conditions, which enables us to precisely establish the law governing the time dependence of OTOCs. Our findings reveal that both C_p and C_T exhibit unbounded quadratic growth, indicating a power law scrambling behavior in their long-term evolutions. The observation of similar time dependence laws for different OTOCs suggests a universality in this power law growth for the QKR model. It is known that the exotic physics exhibited by the QKR model under quantum resonance conditions, such as ballistic energy diffusion and topologically protected transport in momentum space, originates from the essential quantum coherence effects, without classical counterparts. Our findings unveil the role of quantum coherence in facilitating quantum scrambling, a connection of potential significance for applications in quantum information.

The paper is organized as follows. In Section 2, we describe the system and show the quadratic growth of OTOCs. In Section 3, we show our theoretical analysis. A summary is presented in Section 4.

2. Model and Main Results

The dimensionless Hamiltonian of the QKR model reads

$$\mathrm{H} = \frac{p^2}{2} + K\cos(\theta)\sum_n \delta(t - t_n)\,, \tag{1}$$

where $p = -i\hbar_{\mathrm{eff}}\partial/\partial\theta$ is the angular momentum operator, θ is the angle coordinate, with commutation relation $[\theta, p] = i\hbar_{\mathrm{eff}}$. Here, $\hbar_{\mathrm{eff}}$ denotes the effective planck's constant, and K is the kicking strength [55]. One experimental realization of the QKR model involves ultracold atoms exposed to a pulsed laser standing field that mimics a delta-kicking potential [56]. The eigenequation of the angular momentum operator is $p|\varphi_n\rangle = p_n|\varphi_n\rangle$ with an eigenvalue of $p_n = n\hbar_{\mathrm{eff}}$ and eigenstate of $\langle\theta|\varphi_n\rangle = e^{in\theta}/\sqrt{2\pi}$. With the complete basis of $|\varphi_n\rangle$, an arbitrary state can be expanded as $|\psi\rangle = \sum_n \psi_n|\varphi_n\rangle$. One period evolution of the quantum state from t_n to t_{n+1} is governed by $|\psi(t_{n+1})\rangle = U|\psi(t_n)\rangle$. The Floquet operator U involves two components, i.e., $U = U_f U_K$, where the $U_f = \exp\left(-ip^2/2\hbar_{\mathrm{eff}}\right)$ represents the free evolution operator and the kicking term is denoted by $U_K = \exp[-iK\cos(\theta)/\hbar_{\mathrm{eff}}]$.

The OTOCs are defined using the average of the squared commutator, i.e., $C(t) = -\langle[A(t), B]^2\rangle$. Here, both $A(t) = U^\dagger(t)AU(t)$ and B are evaluated in the Heisenberg picture. The average $\langle\cdot\rangle$ refers to the operator's expectation value concerning the initial state $\langle\psi(t_0)|\cdot|\psi(t_0)\rangle$ [29,57–60]. We investigate two distinct OTOCs, one denoted as $C_p = -\langle[p(t), p]^2\rangle$, and the other as $C_T = -\langle[T(t), p]^2\rangle$, where $T = \exp(-i\epsilon p/\hbar_{\mathrm{eff}})$ represents the translation operator. We focus solely on the quantum resonance condition, i.e., $\hbar_{\mathrm{eff}} = 4\pi$. Without loss of generality, we choose an initial state $\psi(\theta, t_0) = \cos(\theta)/\sqrt{\pi}$. Our main findings can be summarized by the following relationships

$$C_p(t) = 12\pi^2K^2t^2\,, \tag{2}$$

and

$$C_T(t) = \sin^2\left(\frac{\epsilon}{2}\right)[2+\cos(\epsilon)]K^2t^2\,. \tag{3}$$

These relations clearly demonstrate the existence of the quadratic growth of different OTOCs.

In order to confirm our above theoretical predictions, we numerically calculate both the C_p and C_T for different Ks. Our results demonstrate that for a specific K (e.g., $K = 1$ in Figure 1), both C_p and C_T increase unboundedly with time. Furthermore, the larger the K, the faster they increase, following perfectly with the relations described in Equations (2) and (3). The continuous, unsaturated growth of OTOCs is attributed to the delocalization mechanism under quantum resonance conditions. When the delocalization mechanism is absent, the process of dynamical localization in quantum non-resonance conditions leads to the saturation of OTOCs, which has been reported in our previous investigation in Ref. [27]. It is noteworthy that the dependency of C_T on the parameter ϵ offers a means of manipulating quantum scrambling by adjusting the translation operator, shedding light on the quantum control of non-Hermitian Floquet systems.

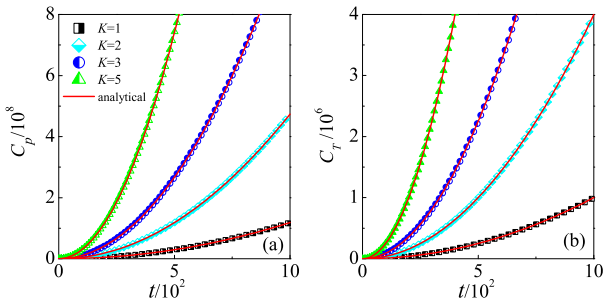

Figure 1. Time dependence of the C_p (**a**) and C_T (**b**) for $K = 1$ (squares), 2 (diamonds), 3 (circles), and 5 (triangles). Red lines in (**a**,**b**) indicate our theoretical prediction in Equations (2) and (3), respectively. In (**b**), the value of the translation parameter is $\epsilon = \pi$.

The quadratic growth in OTOCs also emerges when we use the translation operator $T = \exp(-i\epsilon p/\hbar_{\rm eff})$ and a projection operator onto an initial state $B = |\psi(t_0)\rangle\langle\psi(t_0)|$ for OTOCs. In this situation, one can obtain the relation $C(t) = 1 - \mathcal{F}_O$, with $\mathcal{F}_O = |\langle\psi(t_0)|T|\psi(t_0)\rangle|^2$ being named as fidelity out-of-time-ordered correlators (FOTOCs). Under the condition $\epsilon/\hbar_{\rm eff} \ll 1$, straightforward derivation yields the approximation $C(t) \approx (\epsilon/\hbar_{\rm eff})^2\left[\langle p^2(t)\rangle - \langle p(t)\rangle^2\right]$, by neglecting the terms in the Taylor expansion of $T = \exp(-i\epsilon p/\hbar)$ of orders larger than two. The mean momentum is zero, i.e., $\langle p(t)\rangle = 0$ due to the symmetry of both the specific initial state $\psi(\theta, t_0) = \cos(\theta)/\sqrt{\pi}$ and the kicking potential. Therefore, the OTOCs is proportional to the mean energy, i.e., $C(t) \approx (\epsilon/\hbar_{\rm eff})^2\langle p^2(t)\rangle \approx (\epsilon K t/2\hbar_{\rm eff})^2$, indicating clearly the quadratic growth. Note that the Fourier spectrum of the FOTOCs $\mathcal{F}_O$ can be utilized in constructing the Rényi entropy [61–63]. In fact, FOTOCs have been used to characterize the multiple entanglements among different degrees of freedom in the kicked top model, which can be regarded as a collective of many spins [64]. It is known that the QKR model is a limit of the kicked top model with angular momentum being infinity [65]. This provides the theoretical foundation for the significant implications of the quadratic growth of OTOCs in measuring the buildup of quantum entanglement.

In the atom-optics realization of the QKR model, the experimental constraints in practice often introduce very small detuning from the exact quantum resonance condition [66]. We further consider the effects of the slight variation in the value of $\hbar_{\rm eff}$ from quantum resonance condition, i.e., $\hbar_{\rm eff} = 4\pi + \Delta$ on the quantum scrambling. In this situation, there is a fictitious classical limit in which the parameter Δ plays the role of the effective Planck's constant [66,67]. We should note that traditional definition of the semiclassical limit with $\hbar_{\rm eff}$ tending to zero does not make sense for the resonance case as $\hbar_{\rm eff} = 4\pi$. Our numerical

results show that for a specific Δ (e.g., $\Delta = 0.0025$ in Figure 2a), the C_p follows the quadratic growth of $\Delta = 0$ for finite time duration, i.e., $t < t_c$, after which it fluctuates around a saturation level. Interestingly, the saturate level decreases with the increase in Δ. For sufficiently large Δ (e.g., $\Delta = 0.1$), the C_p remains almost at its initial value and does not increases with time. We further investigate the C_p at a specific time for different Δ. The inset in Figure 2a shows that the $C_p(t = 500)$ decreases with some fluctuations as the absolute value of Δ departs from zero, which demonstrates the suppression of OTOCs by the variation of $\hbar_{\text{eff}}$ from quantum resonance condition. The time evolution of C_T also exhibits the reduction from the quadratic growth in $\Delta = 0$ with the increase in Δ (see Figure 2b). When the $|\Delta|$ increases from zero, the QKR transitions to the quantum non-resonance regime, where the mechanism of dynamical localization suppresses the growth of OTOCs [27].

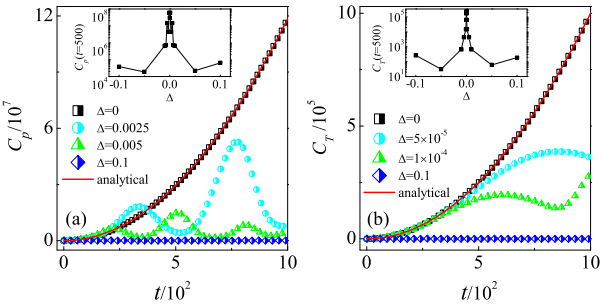

Figure 2. Time dependence of the C_p (**a**) and C_T (**b**) for $K = 1$. In (**a**), $\Delta = 0$ (squares), 0.0025 (circles), 0.005 (triangles), and 0.1 (diamonds). Inset: The C_p at time $t = 500$ versus Δ. In (**b**), $\Delta = 0$ (squares), 5×10^{-5} (circles), 1×10^{-4} (triangles), and 0.1 (diamonds). Inset: The C_T at time $t = 500$ versus Δ. Red lines in (**a**,**b**) indicate our theoretical prediction in Equations (2) and (3), respectively. In (**b**), the value of the translation parameter is $\epsilon = \pi$.

3. Theoretical Analysis

It is straightforward to derive the relation

$$C(t) = C_1(t) + C_2(t) - 2\text{Re}[C_3(t)] \,, \tag{4}$$

where the first two terms on the right side, i.e., two-points correlator, are defined as

$$C_1(t) := \langle A^\dagger(t) B^2 A(t) \rangle = \langle \psi_R(t_0) | B^2 | \psi_R(t_0) \rangle \,, \tag{5}$$

$$C_2(t) := \langle B^\dagger A^\dagger(t) A(t) B \rangle = \langle \varphi_R(t_0) | \varphi_R(t_0) \rangle \,, \tag{6}$$

and the four-point correlator is given by

$$C_3(t) := \langle A^\dagger(t) B A(t) B \rangle = \langle \psi_R(t_0) | B | \varphi_R(t_0) \rangle \,, \tag{7}$$

with $|\psi_R(t_0)\rangle = U^\dagger(t) A U(t) |\psi(t_0)\rangle$ and $|\varphi_R(t_0)\rangle = U^\dagger(t) A U(t) B |\psi(t_0)\rangle$. Here, $\text{Re}[\cdots]$ denotes the real part of the complex variable [29].

The derivation of C_1 at a specific time $t = t_n$ involves three sequential steps [68]. Firstly, evolving the initial state $|\psi(t_0)\rangle$ from t_0 to t_n yields $|\psi(t_n)\rangle = U(t_n, t_0)|\psi(t_0)\rangle$. Secondly, applying operator A to $|\psi(t_n)\rangle$ produces $|\tilde{\psi}(t_n)\rangle = A|\psi(t_n)\rangle$. Finally, the time reversal from t_n to t_0 for $|\tilde{\psi}(t_n)\rangle$ results in $|\psi_R(t_0)\rangle = U^\dagger(t_n, t_0)|\tilde{\psi}(t_n)\rangle$. Equation (5) indicates that C_1 is the expectation value of operator B^2 for $|\psi_R(t_0)\rangle$. The process to derive C_2 at time $t = t_n$ involves four steps. Firstly, applying the operator B to the initial state $|\psi(t_0)\rangle$ yields the state $|\varphi(t_0)\rangle = B|\psi(t_0)\rangle$. Secondly, the forward evolution for the state $|\varphi(t_0)\rangle$ results in a state $|\varphi(t_n)\rangle = U(t_n, t_0)|\varphi(t_0)\rangle$. In the third step, we apply the operator A to the state $|\varphi(t_n)\rangle$, which creates a new state $|\tilde{\varphi}(t_n)\rangle = A|\varphi(t_n)\rangle$. The fourth step involves a time reversal for the state $|\tilde{\varphi}(t_n)\rangle$, giving $|\varphi_R(t_0)\rangle = U^\dagger(t_n, t_0)|\tilde{\varphi}(t_n)\rangle$. The norm of $|\varphi_R(t_0)\rangle$

defines C_2 as shown in Equation (6). With the two states $|\psi_R(t_0)\rangle$ and $|\varphi_R(t_0)\rangle$, we can calculate the C_3 based on Equation (7).

Under the quantum resonance condition $\hbar_{\text{eff}} = 4\pi$, each matrix element of the free evolution operator U_f in angular momentum space equals to unity, i.e., $U_f(n) = \exp(-i2\pi n^2) = 1$. Consequently, the operator has no impact on the time evolution of quantum states. For one period evolution from $t = t_n$ to $t = t_{n+1}$, we only need to use the kicking evolution operator to act on the quantum state, i.e., $|\psi(t_{n+1})\rangle = U_K|\psi(t_n)\rangle$. This leads to an exact expression of a quantum state at arbitrary time $t = t_n$ in angle coordinate space, i.e., $\psi(\theta, t_n) = U_K(\theta, t_n)\psi(\theta, t_0) = \exp[-iKt_n\cos(\theta)/\hbar_{\text{eff}}]\psi(\theta, t_0)$. Based on this, we can derive analytical expressions for both $|\psi_R(t_0)\rangle$ and $|\varphi_R(t_0)\rangle$, which yields the theoretical predictions for the OTOCs $C(t)$.

3.1. Derivation of the C_p

Given the operators $(A = p, B = p)$ and the quantum resonance condition, the three components of the OTOCs C_p are denoted as $C_{p,1}(t) = \langle\psi_R(t_0)|p^2|\psi_R(t_0)\rangle$, $C_{p,2}(t) = \langle\varphi_R(t_0)|\varphi_R(t_0)\rangle$, and $C_{p,3}(t) = \langle\psi_R(t_0)|p|\varphi_R(t_0)\rangle$, with $|\psi_R(t_0)\rangle = U_K^\dagger(t)pU_K(t)|\psi(t_0)\rangle$ and $|\varphi_R(t_0)\rangle = U_K^\dagger(t)pU_K(t)p|\psi(t_0)\rangle$. At the time $t = t_n$, the action the operator p to the state $\psi(\theta, t_n) = U_K(\theta, t_n)\psi(\theta, t_0)$ yields a new state $\tilde{\psi}(\theta, t_n) = p\psi(\theta, t_n) = \sin(\theta)\psi(\theta, t_n)Kt_n - i4\pi\psi^{(1)}(\theta, t_0)\exp[-iKt_n\cos(\theta)/4\pi]$, where superscript (n) $(n = 1, 2\ldots)$ denotes the n-th order derivative of the functions. We then perform the time reversal from t_n to t_0 starting from $\tilde{\psi}(\theta, t_n)$ and obtain

$$\begin{aligned}\psi_R(\theta, t_0) &= [U_K(\theta, t_n)]^\dagger\tilde{\psi}(\theta, t_n)\\ &= Kt_n\sin(\theta)\psi(\theta, t_0) - i4\pi\psi^{(1)}(\theta, t_0)\,.\end{aligned} \tag{8}$$

With this state, one can obtain the analytical expression of $C_{p,1}(t_n)$

$$\begin{aligned}C_{p,1}(t_n) = 16\pi^2K^2t_n^2\int_0^{2\pi}|\Psi(\theta)|^2d\theta\\ + 256\pi^4\int_0^{2\pi}|\psi^{(2)}(\theta, t_0)|^2d\theta\,,\end{aligned} \tag{9}$$

where the function $\Psi(\theta)$ takes the forms $\Psi(\theta) = \psi(\theta, t_0)\cos(\theta) + \psi^{(1)}(\theta, t_0)\sin(\theta)$.

For the derivation of $C_{p,2}(t_n)$, we apply the operator p to acting on the initial state, which yields $\varphi(\theta, t_0) = p\psi(\theta, t_0) = -i4\pi\psi^{(1)}(\theta, t_0)$. Then, forward evolution from t_0 to t_n creates the state $\varphi(\theta, t_n) = -i4\pi\psi^{(1)}(\theta, t_0)\exp[-iKt_n\cos(\theta)/4\pi]$, along with $\tilde{\varphi}(\theta, t_n) = p\varphi(\theta, t_n) = Kt_n\sin(\theta)\varphi(\theta, t_n) - i4\pi\varphi^{(1)}(\theta, t_0)\exp\left[-\frac{i}{4\pi}Kt_n\cos(\theta)\right]$. Conducting the backward evolution from t_n to t_0 for the state $\tilde{\varphi}(\theta, t_n)$, we obtain

$$\varphi_R(\theta, t_0) = Kt_n\sin(\theta)\varphi(\theta, t_0) - i4\pi\varphi^{(1)}(\theta, t_0)\,. \tag{10}$$

With the assistance of the two states, we establish the following relations

$$\begin{aligned}C_{p,2}(t_n) = 16\pi^2K^2t_n^2\int_0^{2\pi}|\psi^{(1)}(\theta, t_0)|^2\sin^2(\theta)d\theta +\\ 256\pi^4\int_0^{2\pi}|\psi^{(2)}(\theta, t_0)|^2d\theta\,,\end{aligned} \tag{11}$$

and

$$\begin{aligned}C_{p,3}(t_n) = -16\pi^2K^2t_n^2\int_0^{2\pi}\Gamma(\theta)d\theta + i64\pi^3Kt_n\int_0^{2\pi}\Upsilon(\theta)d\theta\\ - 256\pi^4\int_0^{2\pi}\left[\psi^{(1)}(\theta, t_0)\right]^*\psi^{(3)}(\theta, t_0)d\theta\,.\end{aligned} \tag{12}$$

Here, the superscript $*$ indicates the complex conjugate of the variable. The functions $\Gamma(\theta)$ and $\Upsilon(\theta)$ take the forms $\Gamma(\theta) = \psi^*(\theta, t_0)\left[\sin^2(\theta)\psi^{(2)}(\theta, t_0) + \frac{1}{2}\sin(2\theta)\psi^{(1)}(\theta, t_0)\right]$ and $\Upsilon(\theta) = \sin(\theta)\left[\psi^*(\theta, t_0)\psi^{(3)}(\theta, t_0) - \left[\psi^{(1)}(\theta, t_0)\right]^*\psi^{(2)}(\theta, t_0)\right] - \cos(\theta)|\psi^{(1)}(\theta, t_0)|^2$. Therefore, we can obtain the expression of the OTOCs

$$\begin{aligned} C_p(t_n) =& C_{p,1}(t_n) + C_{p,2}(t_n) - 2\mathrm{Re}[C_{p,3}(t_n)] \\ =& 16\pi^2 K^2 t_n^2 \int_0^{2\pi} \{\Phi(\theta) + 2\mathrm{Re}[\Gamma(\theta)]\} d\theta \\ &+ 128\pi^3 K t_n \int_0^{2\pi} \mathrm{Im}[\Upsilon(\theta)] d\theta \\ &+ 512\pi^4 \int_0^{2\pi} \mathrm{Re}\left\{\left[\psi^{(1)}(\theta, t_0)\right]^* \psi^{(3)}(\theta, t_0)\right\} d\theta \\ &+ 512\pi^4 \int_0^{2\pi} |\psi^{(2)}(\theta, t_0)|^2 d\theta \,, \end{aligned} \tag{13}$$

with $\Phi(\theta) = |\psi^{(1)}(\theta, t_0)|^2 \sin^2(\theta) + |\Psi(\theta)|^2$ and $\mathrm{Im}(\cdots)$ indicating the imaginary part of a complex variable. It is obvious that the time dependence of C_p contains a quadratic function, determined by the integral of the functions $\Phi(\theta)$ and $\Gamma(\theta)$, and a linear function related to the integral of the function $\Upsilon(\theta)$. The exact dependence of the functions $\Phi(\theta)$, $\Gamma(\theta)$, and $\Upsilon(\theta)$ on initial states, as shown above, serves as a crucial knob for controlling the behavior of OTOCs through the preparation of different starting conditions. For example, suppose we choose the initial state $\psi(\theta, t_0) = \cos(\theta)/\sqrt{\pi}$, resulting in the equivalence

$$C_p(t) = 12\pi^2 K^2 t^2 \,. \tag{14}$$

3.2. Derivation of the C_T

The three components of C_T are represented as $C_{T,1}(t) = \langle\psi_R(t_0)|p^2|\psi_R(t_0)\rangle$, $C_{T,2}(t) = \langle\varphi_R(t_0)|\varphi_R(t_0)\rangle$, and $C_{T,3}(t) = \langle\psi_R(t_0)|p|\varphi_R(t_0)\rangle$. Here, the time-reversed states at time t_0, influenced by the operators $T = \exp(-i\epsilon p/\hbar_{\mathrm{eff}})$ and the initial states $\psi(t_0)$, take the forms $|\psi_R(t_0)\rangle = U_K^\dagger(t)\exp(-i\epsilon p/\hbar_{\mathrm{eff}})U_K(t)|\psi(t_0)\rangle$ and $|\varphi_R(t_0)\rangle = U_K^\dagger(t)\exp(-i\epsilon p/\hbar_{\mathrm{eff}})U_K(t)\exp(-i\epsilon p/\hbar_{\mathrm{eff}})|\psi(t_0)\rangle$, respectively. By repeating the same procedure for the derivation of both $|\psi_R(t_0)\rangle$ and $|\varphi_R(t_0)\rangle$ of C_p, we can obtain the exact expressions of the two states under quantum resonance condition

$$\psi_R(\theta, t_0) = \psi(\theta + \epsilon, t_0)\exp\left[\frac{iKt}{2\pi}\sin\left(\frac{\epsilon}{2}\right)\sin\left(\frac{2\theta + \epsilon}{2}\right)\right] \tag{15}$$

and

$$\varphi_R(\theta, t_0) = -i4\pi\psi^{(1)}(\theta + \epsilon, t_0)\exp\left[\frac{iKt}{2\pi}\sin\left(\frac{\epsilon}{2}\right)\sin\left(\frac{2\theta + \epsilon}{2}\right)\right]. \tag{16}$$

Consequently, one can derive analytically the three components of the C_T

$$\begin{aligned} C_{T,1}(t) =& 4K^2t^2\sin^2\left(\frac{\epsilon}{2}\right)\int_0^{2\pi}\cos^2\left(\theta + \frac{\epsilon}{2}\right)|\psi(\theta + \epsilon, t_0)|^2 d\theta \\ &+ 16\pi^2\int_0^{2\pi}\left|\psi^{(1)}(\theta + \epsilon, t_0)\right|^2 d\theta \,, \end{aligned} \tag{17}$$

$$C_{T,2}(t) = 16\pi^2\int_0^{2\pi}\left|\psi^{(1)}(\theta + \epsilon, t_0)\right|^2 d\theta \,, \tag{18}$$

and

$$\begin{aligned} C_{T,3}(t) =& -i8\pi\sin\left(\frac{\epsilon}{2}\right)Kt\int_0^{2\pi} v(\theta)d\theta \\ &- 16\pi^2\int_0^{2\pi}\psi^*(\theta + \epsilon, t_0)\psi^{(2)}(\theta + \epsilon, t_0)d\theta \,. \end{aligned} \tag{19}$$

with $v(\theta) = \psi^*(\theta+\epsilon, t_0)\psi^{(1)}(\theta+\epsilon, t_0)\cos(\theta+\frac{\epsilon}{2})$. Combining these three parts yields

$$\begin{aligned} C_T(t) =& C_{T,1}(t) + C_{T,2}(t) - 2\mathrm{Re}[C_{T,3}(t)] \\ =& 4K^2t^2\sin^2\left(\frac{\epsilon}{2}\right)\int_0^{2\pi}\cos^2\left(\theta+\frac{\epsilon}{2}\right)|\psi(\theta+\epsilon,t_0)|^2 d\theta \\ & - 16\pi\sin\left(\frac{\epsilon}{2}\right)Kt\int_0^{2\pi}\mathrm{Im}[v(\theta)]d\theta\,, \\ & + 32\pi^2\int_0^{2\pi}\mathrm{Re}\left[\psi^*(\theta+\epsilon,t_0)\psi^{(2)}(\theta+\epsilon,t_0)\right]d\theta\,, \\ & + 32\pi^2\int_0^{2\pi}\left|\psi^{(1)}(\theta+\epsilon,t_0)\right|^2 d\theta\,. \end{aligned} \tag{20}$$

Obviously, the term of quadratic growth in the function C_T is governed by the integral involving the modular square $|\psi(\theta+\epsilon, t_0)|^2$. The term of the linear growth in C_T depends on the integral of the function $v(\theta)$, which is related to the initial state $\psi(\theta, t_0)$. The close relationship between C_T and the initial state provides the unique opportunity to engineer the OTOCs' behavior under various initial states. For a specific form of the initial state $\psi(\theta, t_0) = \cos(\theta)/\sqrt{\pi}$, it is straightforward to establish the relation

$$C_T(t) = \sin^2\left(\frac{\epsilon}{2}\right)[2+\cos(\epsilon)]K^2t^2\,. \tag{21}$$

4. Conclusions and Discussion

In this work, we thoroughly investigate the dynamics of OTOCs, employing C_p and C_T under quantum resonance conditions. The C_p quantifies the commutation relation of two angular momentum operators at different times, while the C_T measures that between the translation operator and angular momentum operator at different times. Our exact deductions of the quantum states during forward evolution and time reversal under quantum resonance allow us to establish the laws governing the time dependence of OTOCs. Our findings demonstrate that both C_p and C_T exhibit quadratic growth with time evolution, revealing an intrinsic power-law scrambling in their late-time behavior. Note that the mechanism of dynamical localization under non-resonant conditions suppresses quantum scrambling [27]. Therefore, the observed quadratic growth of OTOCs finds its origin in essential quantum coherence effects arising from quantum resonance, without classical analogs. We expect that the identification of similar power laws for different types of OTOCs reveals the universality in the power-law growth within the QKR model. It has been found that the delocalization effects with unique quantum coherence leads to the quadratic growth of OTOCs in the QKR model with quantum non-resonance condition [7]. Therefore, our discovery of the crucial role played by quantum coherence in facilitating quantum scrambling has significant implications in the fields of quantum information and quantum chaos [6,8,63].

Author Contributions: Investigation, G.L.; Writing—review & editing, W.Z. All authors have read and agreed to the published version of the manuscript.

Funding: This work is supported by the National Natural Science Foundation of China (Grant Nos. 12065009 and 12365002), the Natural Science Foundation of Jiangxi province (Grant Nos. 20224ACB201006 and 20224BAB201023).

Institutional Review Board Statement: Not applicable.

Data Availability Statement: No new data were created or analyzed in this study. Data sharing is not applicable to this article.

Conflicts of Interest: The authors declare no conflict of interest.

References

1. Yan, B.; Cincio, L.; Zurek, W.H. Information Scrambling and Loschmidt Echo. *Phys. Rev. Lett.* **2020**, *124*, 160603. [CrossRef]
2. Yan, B.; Sinitsyn, N.A. Recovery of Damaged Information and the Out-of-Time-Ordered Correlators. *Phys. Rev. Lett.* **2020**, *125*, 040605. [CrossRef]
3. Wang, J.H.; Cai, T.Q.; Han, X.Y.; Ma, Y.W.; Wang, Z.L.; Bao, Z.H.; Li, Y.; Wang, H.Y.; Zhang, H.Y.; Sun, L.Y.; et al. Information scrambling dynamics in a fully controllable quantum simulator. *Phys. Rev. Res.* **2022**, *4*, 043141. [CrossRef]
4. Swingle, B. Unscrambling the physics of out-of-time-order correlators. *Nat. Phys.* **2018**, *14*, 988. [CrossRef]
5. Omanakuttan, S.; Chinni, K.; Blocher, P.D.; Poggi, P.M. Scrambling and quantum chaos indicators from long-time properties of operator distributions. *Phys. Rev. A* **2023**, *107*, 032418. [CrossRef]
6. García-Mata, I.; Jalabert, R.A.; Wisniacki, D.A. Out-of-time-order correlators and quantum chaos. *Scholarpedia* **2023**, *18*, 55237. [CrossRef]
7. Hamazaki, R.; Fujimoto, K.; Ueda, M. Operator Noncommutativity and Irreversibility in Quantum Chaos. *arXiv* **2018**, arXiv:1807.02360.
8. Varikuti, N.D.; Sahu, A.; Lakshminarayan, A.; Madhok, V. Probing dynamical sensitivity of a non-Kolmogorov-Arnold-Moser system through out-of-time-order correlators. *Phys. Rev. E* **2024**, *109*, 014209. [CrossRef]
9. Sreeram, P.G.; Vaibhav, M.; Arul, L. Out-of-time-ordered correlators and the Loschmidt echo in the quantum kicked top: how low can we go? *J. Phys. D Appl. Phys.* **2021**, *54*, 274004.
10. Zhao, S.K.; Ge, Z.Y.; Xiang, Z.C.; Xue, G.M.; Yan, H.S.; Wang, Z.T.; Wang, Z.; Xu, H.K.; Su, F.F.; Yang, Z.H.; et al. Probing Operator Spreading via Floquet Engineering in a Superconducting Circuit. *Phys. Rev. Lett.* **2022**, *129*, 160602. [CrossRef]
11. Dağ, C.B.; Sun, K.; Duan, L.M. Detection of Quantum Phases via Out-of-Time-Order Correlators. *Phys. Rev. Lett.* **2019**, *123*, 140602. [CrossRef]
12. Zamani, S.; Jafari, R.; Langari, A. Out-of-time-order correlations and Floquet dynamical quantum phase transition. *Phys. Rev. B* **2022**, *105*, 094304. [CrossRef]
13. Omanakuttan, S.; Lakshminarayan, A. Out-of-time-ordered correlators and quantum walks. *Phys. Rev. E* **2019**, *99*, 062128. [CrossRef] [PubMed]
14. Yin, C.; Lucas, A. Quantum operator growth bounds for kicked tops and semiclassical spin chains. *Phys. Rev. A* **2021**, *103*, 042414. [CrossRef]
15. Zhang, P.F.; Yu, Z.H. Dynamical Transition of Operator Size Growth in Quantum Systems Embedded in an Environment. *Phys. Rev. Lett.* **2023**, *130*, 250401. [CrossRef] [PubMed]
16. Liu, F.L.; Garrison, J.R.; Deng, D.L.; Gong, Z.X.; Gorshkov, A.V. Asymmetric Particle Transport and Light-Cone Dynamics Induced by Anyonic Statistics. *Phys. Rev. Lett.* **2018**, *121*, 250404. [CrossRef] [PubMed]
17. Das, A.; Chakrabarty, S.; Dhar, A.; Kundu, A.; Huse, D.A.; Moessner, R.; Ray, S.S.; Bhattacharjee, S. Light-Cone Spreading of Perturbations and the Butterfly Effect in a Classical Spin Chain. *Phys. Rev. Lett.* **2018**, *121*, 024101. [CrossRef]
18. Keselman, A.; Nie, L.; Berg, E. Scrambling and Lyapunov exponent in spatially extended systems. *Phys. Rev. B* **2021**, *103*, L121111. [CrossRef]
19. Mezei, M.; Sárosi, G. Chaos in the butterfly cone. *J. High Energy Phys.* **2020**, *01*, 186. [CrossRef]
20. Pappalardi, S.; Kurchan, J. Quantum bounds on the generalized lyapunov exponents. *Entropy* **2023**, *25*, 246. [CrossRef]
21. MacCormack, I.; Tan, M.T.; Kudler-Flam, J.; Ryu, S. Operator and entanglement growth in nonthermalizing systems: Many-body localization and the random singlet phase. *Phys. Rev. B* **2021**, *104*, 214202. [CrossRef]
22. Kobrin, B.; Yang, Z.; Kahanamoku-Meyer, G.D.; Olund, C.T.; Moore, J.E.; Stanford, D.; Yao, N.Y. Many body chaos in the Sachdev-Ye-Kitaev model. *Phys. Rev. Lett.* **2021**, *126*, 030602. [CrossRef] [PubMed]
23. Bilitewski, T.; Bhattacharjee, S.; Moessner, R. Classical many-body chaos with and without quasiparticles. *Phys. Rev. B* **2021**, *103*, 174302. [CrossRef]
24. Xu, T.R.; Scaffidi, T.; Cao, X.Y. Does Scrambling Equal Chaos? *Phys. Rev. Lett.* **2020**, *124*, 140602. [CrossRef]
25. Jaiswal, N.; Gautam, M.; Gill, A.; Sarkar, T. Fotoc complexity in the Lipkin-Meshkov-Glick model and its variant. *Eur. Phys. J. B* **2024**, *97*, 5. [CrossRef]
26. Huh, K.-B.; Ikeda, K.; Jahnke, V.; Kim, K.-Y. Diagnosing first- and second-order phase transitions with probes of quantum chaos. *Phys. Rev. E* **2021**, *104*, 024136. [CrossRef]
27. Zhao, W.L.; Wang, R.R.; Ke, H.; Liu, J. Scaling laws of the out-of-time-order correlators at the transition to the spontaneous PT-symmetry breaking in a Floquet system. *Phys. Rev. A* **2023**, *107*, 062201. [CrossRef]
28. Zhao, W.L.; Liu, J. Superexponential behaviors of out-of-time ordered correlators and Loschmidt echo in a non-Hermitian interacting system. *arXiv* **2023**, arXiv:2305.1215.
29. Zhao, W.L.; Hu, Y.; Li, Z.; Wang, Q. Super-exponential growth of Out-of-time-ordered correlators. *Phys. Rev. B* **2021**, *103*, 184311. [CrossRef]
30. Qi, Z.; Scaffidi, T.; Cao, X. Surprises in the deep Hilbert space of all-to-all systems: From superexponential scrambling to slow entanglement growth. *Phys. Rev. B* **2023**, *108*, 054301. [CrossRef]
31. Santhanam, M.S.; Paul, S.; Kannan, J.B. Quantum kicked rotor and its variants: Chaos, localization and beyond. *Phys. Rep.* **2022**, *956*, 1. [CrossRef]
32. Wang, J.; García-García, A.M. Anderson transition in a three-dimensional kicked rotor. *Phys. Rev. E* **2009**, *79*, 036206. [CrossRef]

33. Scoquart, T.; Wellens, T.; Delande, D.; Cherroret, N. Quench dynamics of a weakly interacting disordered Bose gas in momentum space. *Phys. Rev. Res.* **2020**, *2*, 033349. [CrossRef]
34. Ho, D.Y.H.; Gong, J.B. Quantized Adiabatic Transport In Momentum Space. *Phys. Rev. Lett.* **2012**, *109*, 010601. [CrossRef] [PubMed]
35. Cheng, Q.Q.; Pan, Y.M.; Wang, H.Q.; Zhang, C.S.; Yu, D.; Gover, A.; Zhang, H.J.; Li, T.; Zhou, L.; Zhu, S.N. Observation of Anomalous π Modes in Photonic Floquet Engineering. *Phys. Rev. Lett.* **2019**, *122*, 173901. [CrossRef] [PubMed]
36. Zhou, L.W.; Zhang, D.J. Non-Hermitian Floquet Topological Matter—A Review. *Entropy* **2023**, *25*, 1401. [CrossRef]
37. Zhou, L.W. Entanglement spectrum and entropy in Floquet topological matter. *Phys. Rev. Res.* **2022**, *4*, 043164. [CrossRef]
38. Wang, H.L.; Wang, J.; Guarneri, I.; Casati, G.; Gong, J.B. Exponential quantum spreading in a class of kicked rotor systems near high-order resonances. *Phys. Rev. E* **2013**, *88*, 052919. [CrossRef] [PubMed]
39. Wang, J.; Gong, J.B. Proposal of a cold-atom realization of quantum maps with Hofstadter's butterfly spectrum. *Phys. Rev. A* **2008**, *77*, 031405(R). [CrossRef]
40. Wang, J.; Gong, J.B. Generating a fractal butterfly Floquet spectrum in a class of driven SU(2) systems. *Phys. Rev. E* **2010**, *81*, 026204. [CrossRef]
41. Wang, H.L.; Ho, D.Y.H.; Lawton, W.; Wang, J.; Gong, J.B. Kicked-Harper model versus on-resonance double-kicked rotor model: From spectral difference to topological equivalence. *Phys. Rev. E* **2013**, *88*, 052920. [CrossRef]
42. Faddeev, L.D.; Kashaev, R.M. Generalized Bethe ansatz equations for Hofstadter problem. *Commun. Math. Phys.* **1995**, *169*, 181. [CrossRef]
43. Ikeda, K. Hofstadter's butterfly and Langlands duality. *J. Math. Phys.* **2018**, *59*, 061704. [CrossRef]
44. Kohmoto, M.; Sedrakyan, A. Hofstadter problem on the honeycomb and triangular lattices: Bethe ansatz solution. *Phys. Rev. B* **2006**, *73*, 235118. [CrossRef]
45. Bomantara, R.W.; Raghava, G.N.; Zhou, L.W.; Gong, J.B. Floquet topological semimetal phases of an extended kicked Harper model. *Phys. Rev. E* **2016**, *93*, 022209. [CrossRef]
46. Zhou, L.W. Floquet Second-Order Topological Phases in Momentum Space. *Nanomaterials* **2021**, *11*, 1170. [CrossRef]
47. Chen, Y.; Tian, C.S. Planck's Quantum-Driven Integer Quantum Hall Effect in Chaos. *Phys. Rev. Lett.* **2014**, *113*, 216802. [CrossRef]
48. Tian, C.S.; Chen, Y.; Wang, J. Emergence of integer quantum Hall effect from chaos. *Phys. Rev. B* **2016**, *93*, 075403. [CrossRef]
49. Summy, G.; Wimberger, S. Quantum random walk of a Bose–Einstein condensate in momentum space. *Phys. Rev. A* **2016**, *93*, 023638. [CrossRef]
50. Dadras, S.; Gresch, A.; Groiseau, C.; Wimberger, S.; Summy, G.S. Quantum Walk in Momentum Space with a Bose–Einstein Condensate. *Phys. Rev. Lett.* **2018**, *121*, 070402. [CrossRef] [PubMed]
51. Weiß, M.; Groiseau, C.; Lam, W.K.; Burioni, R.; Vezzani, A.; Summy, G.S.; Wimberger, S. Steering random walks with kicked ultracold atoms. *Phys. Rev. A* **2015**, *92*, 033606. [CrossRef]
52. Dadras, S.; Gresch, A.; Groiseau, C.; Wimberger, S.; Summy, G.S. Experimental realization of a momentum-space quantum walk. *Phys. Rev. A* **2019**, *99*, 043617. [CrossRef]
53. Delvecchio, M.; Groiseau, C.; Petiziol, F.; Summy, G.S.; Wimberger, S. Quantum search with a continuous-time quantum walk in momentum space. *J. Phys. B At. Mol. Opt. Phys.* **2020**, *53*, 065301. [CrossRef]
54. Vakulchyk, I.; Fistul, M.V.; Flach, S. Wave Packet Spreading with Disordered Nonlinear Discrete-Time Quantum Walks. *Phys. Rev. Lett.* **2019**, *122*, 040501. [CrossRef]
55. Casati, G.; Ford, J. Stochastic Behavior in Classical and Quantum Hamiltonian Systems. *Lect. Notes Phys.* **1979**, *93*, 770692.
56. Moore, F.L.; Robinson, J.C.; Bharucha, C.F.; Sundaram, B.; Raizen, M.G. Atom optics realization of the quantum δ-kicked rotor. *Phys. Rev. Lett.* **1995**, *75*, 4598. [CrossRef]
57. Li, J.; Fan, R.H.; Wang, H.Y.; Ye, B.T.; Zeng, B.; Zhai, H.; Peng, X.H.; Du, J.F. Measuring out-of-time-order correlators on a nuclear magnetic resonance quantum simulator. *Phys. Rev. X* **2017**, *7*, 031011. [CrossRef]
58. Hashimoto, K.; Murata, K.; Yoshii, R. Out-of-time-order correlators in quantum mechanics. *J. High Energ. Phys.* **2017**, *10*, 138. [CrossRef]
59. García-Mata, I.; Saraceno, M.; Jalabert, R.A.; Roncaglia, A.J.; Wisniacki, D.A. Chaos signatures in the short and long time behavior of the out-of-time ordered correlator. *Phys. Rev. Lett.* **2018**, *121*, 210601. [CrossRef]
60. Zonnios, M.; Levinsen, J.; Parish, M.M.; Pollock, F.A.; Modi, K. Signatures of Quantum Chaos in an Out-of-Time-Order Tensor. *Phys. Rev. Lett.* **2022**, *128*, 150601. [CrossRef] [PubMed]
61. Fan, R.H.; Zhang, P.F.; Shen, H.T.; Zhai, H. Out-of-Time Order Correlation for Many-Body Localization. *Sci. Bull.* **2017**, *62*, 707. [CrossRef]
62. Lewis-Swan, R.J.; Safavi-Naini, A.; Bollinger, J.J.; Rey, A.M. Unifying scrambling, thermalization and entanglement through measurement of fidelity out-of-timeorder correlators in the Dicke model. *Nat. Commun.* **2019**, *10*, 1581. [CrossRef]
63. Gärttner, M.; Hauke, P.; Rey, A.M. Relating Out-of-Time-Order Correlations to Entanglement via Multiple-Quantum Coherences. *Phys. Rev. Lett.* **2018**, *120*, 040402. [CrossRef]
64. Li, S.C.; Pezzè, L.; Smerzi, A. Multiparticle entanglement dynamics of quantum chaos in a Bose–Einstein condensate. *Phys. Rev. A* **2021**, *103*, 052417. [CrossRef]
65. Haake, F.; Shepelyansky, D.L. The kicked rotator as a limit of the kicked top. *Europhys. Lett.* **1988**, *5*, 671. [CrossRef]

66. Wimberger, S.; Guarneri, I.; Fishman, S. Quantum resonances and decoherence for delta-kicked atoms. *Nonlinearity* **2003**, *16*, 1381. [CrossRef]
67. Wimberger, S.; Guarneri, I.; Fishman, S. Classical Scaling Theory of Quantum Resonances. *Phys. Rev. Lett.* **2004**, *92*, 084102. [CrossRef]
68. Zhao, W.L.; Liu, J. Quantum criticality at the boundary of the non-Hermitian regime of a Floquet system. *arXiv* **2023**, arXiv:2307.00462.